Discovery of CO_2 Ice and Leading-Trailing Spectral Asymmetry on the Uranian Satellite Ariel

W.M. Grundy[1]

Lowell Observatory, 1400 W. Mars Hill Rd., Flagstaff AZ 86001

grundy@lowell.edu

L.A. Young[1] and E.F. Young

Southwest Research Institute, 1050 Walnut St., Boulder CO 80302

[1]Visiting Astronomer at the Infrared Telescope Facility, which is operated by the University of Hawaii under contract from the National Aeronautics and Space Administration

— Submitted to *Icarus* —

Received 2002/09/16 ; accepted _____

Primary contact: Will Grundy

E-mail: *grundy@lowell.edu*

Voice: 928-774-3358

Fax: 928-774-6296

Running head: Ariel's Ices

Manuscript pages: 24

Figures: 3

Tables: 0

ABSTRACT

New 0.8 to 2.4 μm spectral observations of the leading and trailing hemispheres of the Uranian satellite Ariel were obtained at IRTF/SpeX during 2002 July 16 and 17 UT. The new spectra reveal contrasts between Ariel's leading and trailing hemispheres, with the leading hemisphere presenting deeper H_2O ice absorption bands. The observed dichotomy is comparable to leading-trailing spectral asymmetries observed among Jovian and Saturnian icy satellites. More remarkably, the trailing hemisphere spectrum exhibits three narrow CO_2 ice absorption bands near 2 μm. This discovery of CO_2 ice on one hemisphere of Ariel is its first reported detection in the Uranian system.

Subject headings: Ices; satellite surfaces; satellites of Uranus; infrared observations

1. Introduction

Near-infrared spectral differences between leading and trailing hemispheres of tidally-locked Jovian and Saturnian icy satellites have been studied for many years (e.g., Clark *et al.* 1984; Calvin and Clark 1993). Characteristic features include deeper 1.5 and 2 μm H_2O ice absorption bands on leading hemispheres and distorted band shapes on trailing hemispheres (e.g., Grundy *et al.* 1999).

Two processes are thought to be primary causes of the compositional and textural differences which are implied by the observed near-infrared spectral contrasts between leading and trailing hemispheres. First, the orbital motion of tidally-locked satellites around their primary planets results in higher rates of impacts on their leading hemispheres by material from outside the planet-satellite system. Elevated rates of bombardment on leading

hemispheres are compounded by higher mean impact velocities (e.g., Zahnle *et al.* 2001). Second, charged particles in a planet's magnetosphere are dragged around the planet by the rotation of its magnetic field. Since the spin periods of giant planets in our solar system are generally shorter than the orbital periods of their major satellites, magnetospheric particles having gyroradii smaller than the satellites tend to impinge on the trailing hemispheres of the satellites (e.g., Pospieszalska and Johnson 1989; Johnson 1990). Both processes are capable of altering the textures and compositions of icy satellite surfaces, and are thought to account for most observed leading-trailing spectral reflectance dichotomies (apart from unusual cases like Iapetus).

In addition to the well-known spectral asymmetries among Jovian and Saturnian icy satellites, tentative evidence has been reported for leading-trailing spectral asymmetries on Neptune's satellite Triton (Cruikshank and Apt 1984) and Pluto's satellite Charon (Buie and Grundy 2000; Dumas *et al.* 2001). However, near-infrared spectral asymmetries have not previously been seen among Uranian satellites. During the previous two decades of infrared spectral observation, the Uranian system had been oriented roughly pole-on to the sun and Earth, making it difficult for Earth-based observers to study leading and trailing hemispheres separately. Sub-solar latitudes in the Uranian system have recently moved to within 20° of the equator, making searches for leading-trailing asymmetries timely.

The first target we selected for this search was the satellite Ariel. Its orbital period of 2.52 days makes nearly opposite hemispheres conveniently observable on consecutive nights. During the 1986 flyby of Voyager 2, only southern latitudes of Ariel could be viewed. Nevertheless, the Voyager images revealed clear differences between Ariel's leading and trailing hemispheres at visible wavelengths. Younger terrains including bright ejecta deposits were prominent on the southern part of Ariel's leading hemisphere, while the southern part of the trailing hemisphere featured fewer high-albedo patches and had a

slightly redder visual color (e.g., Smith *et al.* 1986; Plescia 1987; Buratti and Mosher 1991; Croft and Soderblom 1991; Veverka *et al.* 1991). Ariel's 5.5 km s^{-1} mean orbital speed around Uranus is sufficient to cause significant differences between cratering rates on leading and trailing hemispheres (e.g., Zahnle *et al.* 2001). The Uranian plasma environment is rather peculiar, compared with Jovian and Saturnian magnetospheres, because of Uranus' very high obliquity and the considerable tilt of Uranus' magnetic dipole with respect to the planet's spin axis (e.g., Ness *et al.* 1986). However, fluxes of energetic protons observed during the Voyager encounter in 1986 are sufficient to drive radiolytic chemistry on time scales much shorter than the age of the solar system (e.g., Bridge *et al.* 1986; Krimigis *et al.* 1986; Lanzerotti *et al.* 1987; Johnson 1990). These factors made a search for spectral dichotomies on Ariel particularly compelling.

2. Observations and Reduction

We observed Ariel during 2002 July 16 11:15-15:08 UT and 2002 July 17 11:51-15:12 UT with the SpeX spectrograph (Rayner *et al.* 1998) at NASA's Infrared Telescope Facility (IRTF). Using the short cross-dispersed mode with a 0.5 arcsec slit we recorded five spectral orders, collectively covering the 0.8 to 2.4 μm wavelength range. Total on-target integration time was 140 minutes on July 16 and 112 minutes on July 17, at airmasses between 1.19 and 1.50. Thin cirrus was present both nights. At the weighted mid-times of the observations (13:08 on July 16, 13:29 on July 17), sub-Earth longitudes on Ariel were 294.6° and 79.5° respectively (IAU coordinates). Sub-Earth latitudes were $-20°$ both nights and sun-object-Earth phase angles were 1.65° and 1.60°. Ariel was 20.00 AU from the sun both nights, and approximately 11 arcsec from the limb of Uranus, far enough for scattered light from Uranus to be negligible.

To record background flux without sacrificing on-target exposure time we observed

alternately in two positions ('A' and 'B') separated by 10 arcsec along the 15 arcsec slit. During our observations, we used an image rotator to orient the slit within 30 degrees of the parallactic angle (the sky-plane projection of the plane defined by observer-object and observer-zenith vectors) to minimize light losses from atmospheric dispersion, taking care to avoid placing Uranus or other moons in the slit. The dispersion caused by the Earth's atmosphere is less than 0.25 arcsec across the slit and 0.43 arcsec in the along-slit direction for the full spectral range, 0.8 to 2.4 μm. For the primary region of interest, 1.25 to 2.4 μm, the dispersions reduce to 0.10 arcsec cross-slit and 0.17 arcsec along-slit. Because the seeing was approximately 0.7 to 1.0 arcsec on both nights, we do not expect atmospheric dispersion to have introduced appreciable slopes in our extracted spectra.

Spectral extraction was accomplished using the Horne (1986) optimal extraction algorithm as implemented by M.W. Buie at Lowell Observatory (e.g., Buie and Grundy 2000; Grundy and Buie 2002).

Between 0.8 and 2.4 μm, the flux from Ariel is entirely due to reflected sunlight. The solar flux distribution was characterized using solar analogs HD219018, 16 Cyg B, and SA112-1333, observed repeatedly at multiple airmasses. At our wavelength range, spectral resolution, and signal precision, the spectra of these stars are indistinguishable from that of the sun. Telluric extinction was determined from the suite of solar analog observations. All stellar and Ariel spectra were corrected to a common airmass prior to performing the ratio between grand average of Ariel and grand average of all the solar analogs, thus removing the solar flux distribution and the instrumental response function. Residual telluric features remain, primarily near 1.4 and 1.9 μm, where telluric H_2O vapor absorptions make sky transparency especially variable both in time and in wavelength.

Wavelength calibration was derived from regular observations of SpeX's internal integrating sphere, illuminated by an argon arc lamp. This source provided from 6 to more

than 20 emission lines per spectral order. Dispersion ranged from 2.3×10^{-4} μm/pixel at the shortest wavelengths to 5.4×10^{-4} μm/pixel in the K band. Internal flexure produced shifts of as much as a pixel, resulting in an uncertainty in wavelength calibration of about ±0.5 pixel. Averaging several arc lamp images together enabled us to determine the effective line spread function for a filled slit for observations spanning a range of positions on the sky. The resulting emission line profiles were well approximated by Gaussians having full width at half maximum (FWHM) of 4 pixels, implying resolving power ($\lambda/\Delta\lambda$) ranging from 870 at 0.8 μm to 1100 at 2.4 μm. With seeing disks uniformly wider than the slit, the filled slit resolution and wavelength uncertainties apply to our observations of solar analogs and Ariel alike. Final, normalized albedo spectra of Ariel for the two nights are shown in Fig. 1.

EDITOR: Please place FIGURE 1 near here.

3. Discussion

The most prominent features in Ariel's near-infrared spectrum are water ice vibrational absorption bands at 1.5, 1.56, 1.65, and 2 μm. Using lower resolution data, these H_2O bands have been analyzed previously (e.g., Cruikshank and Brown 1981; Brown and Cruikshank 1983; Grundy *et al.* 1999). The shapes of the H_2O ice bands in our data are consistent with multiple scattering by ice particles in the 10 to 100 μm size range, in combination with dark material to reduce the overall albedo. The presence of 1.56 and 1.65 μm bands in our data (and also in the data of Grundy *et al.* 1999) clearly indicates that the H_2O is crystalline rather than amorphous, but we cannot determine if it is predominantly hexagonal ice I_h or cubic ice I_c. Based on their far infrared spectral behavior, ice I_h is not expected to differ dramatically from ice I_c in the near infrared, (e.g., Bertie and Whalley 1964; Bertie and Jacobs 1977; Grundy *et al.* 1999), but near infrared laboratory studies of ice I_c have yet to

be published.

The relative strengths and wavelengths of H_2O ice absorption bands have been shown to depend on the temperature of the ice, in addition to the degree of crystallization (e.g., Kieffer and Smythe 1974; Fink and Larson 1975; Grundy and Schmitt 1998). Grundy *et al.* (1999) made use of this dependence to determine an average ice temperature for Ariel of 59±12 K, based on observations obtained in 1995, when the sub-solar latitude was −50°. Using their technique, we now calculate ice temperatures 71±5 and 70±23 K for leading and trailing hemispheres, respectively. The uncertainty is much higher for the trailing hemisphere not because of any difference in the quality of the data obtained, but apparently because the ice absorption band shapes are not as well fit by simple multiple scattering models making use of optical constants for crystalline H_2O ice. The temperature-sensing technique can be vulnerable to the existence of other phases including radiation-damaged, amorphous ice, as discussed by Grundy *et al.* (1999). The primary advantage of this technique is its sensitivity to the brightest, coldest H_2O ice, in contrast with thermal emission measurements which are more sensitive to warmer, darker regions.

As seen in Fig. 1, the 1.5 and 2 μm water ice bands are significantly deeper in the 2002 July 17 UT spectrum, compared with that of 2002 July 16. The 1.5 μm band, for example, was about 65% deeper on July 17. The sub-viewer and sub-solar longitudes on July 17 were ∼80°, corresponding approximately to Ariel's leading hemisphere, which is centered on 90°. On July 16, our ∼295° sub-viewer and sub-solar longitudes were approximately aligned with the opposite, trailing hemisphere, which is centered at 270° longitude. The sub-viewer and sub-solar latitudes on both nights were about −20° (IAU South is oriented in the direction of Ariel's angular momentum vector), much closer to the equator than has been seen over the previous two decades of infrared observation, making these observations more sensitive to hemispherical differences than observations during the 1980s and 1990s.

Deeper H_2O ice bands on leading hemispheres are the norm among icy satellites of Jupiter and Saturn (e.g., Clark *et al.* 1984; Grundy *et al.* 1999), so it is not surprising to now discover the same trend on a Uranian satellite. It is not clear if the deeper leading hemisphere H_2O bands are due to relatively clean ice being excavated by impacts or if the weaker trailing hemisphere bands are due to charged particle sputtering removal of ice. Lanzerotti *et al.* (1987) estimated that $\sim$3 μm of H_2O ice could be removed from Ariel's surface by charged particle sputtering in 10^7 years, though it has yet to be established that the plasma measurements made by Voyager 2 are similar to seasonally-averaged fluxes in the Uranian magnetosphere. Ultraviolet sputtering, which would affect leading and trailing hemispheres equally, may be even more efficient at removing H_2O from Ariel's surface, and micrometeorite sputtering, which would predominantly affect the leading hemisphere, may be most efficient of all (e.g., Eviatar and Johnson 1986; Cheng *et al.* 1991). The observed dichotomy in H_2O ice band depths seems most likely to be the result of a combination of impact- and radiation-related processes.

The appearance of three narrow absorption bands at 1.966, 2.012, and 2.070 μm is more remarkable, since they have not previously been detected on any icy satellite other than Triton (Cruikshank *et al.* 1993). This triplet can be confidently attributed to absorption by the $2\nu_1+\nu_3$, $\nu_1+2\nu_2+\nu_3$, and $4\nu_2+\nu_3$ transitions in CO_2 ice, as shown in Fig. 2 (band identifications from Quirico and Schmitt 1997). Triton's CO_2 bands have been modeled as arising from a mixture of H_2O and CO_2 ices covering approximately 45% of Triton's visible hemisphere (Quirico *et al.* 1999). While the appearance of the CO_2 ice triplet near 2 μm is apparently rare among icy satellites, the much stronger ν_3 fundamental band of CO_2 at 4.25 μm has been detected by the Galileo spacecraft on Jovian satellites Ganymede and Callisto (e.g., McCord *et al.* 1997, 1998; Hibbitts *et al.* 2000). The ν_3 band of CO_2 ice could well exist in the spectra of many icy satellites, as very little CO_2 is required to produce it, but the opacity of telluric CO_2 vapor makes this band impossible to detect from Earth-based

observatories. We are only aware of one earlier, unpublished search for CO_2 ice absorptions on Uranian satellites. A.S. Rivkin, D.E. Trilling, and R.H. Brown surveyed the Uranian satellites in 1998 using the CGS4 spectrometer at the United Kingdom InfraRed Telescope (A.S. Rivkin, personal communication 2002). Rivkin *et al.* did not detect CO_2, though in light of our results, it appears that their non-detection on Ariel resulted from observing the leading rather than trailing hemisphere (Ariel's subsolar longitude was approximately 140° at the time of their observations).

EDITOR: Please place FIGURE 2 near here.

This discovery of CO_2 ice on Ariel's trailing hemisphere doubles the inventory of known ices in the Uranian system. It also raises many interesting questions. For instance, why has CO_2 ice only been seen on Ariel and not on the other major Uranian satellites, and why only on the trailing hemisphere, when H_2O ice bands are normally deeper on leading hemispheres? How abundant and widespread is it, relative to H_2O ice? How long does it survive on Ariel's surface? What processes act on exposed CO_2 ice? Is it a relic of Ariel's primordial volatile inventory? Was it delivered by more recent impactors? Or is it produced from other materials in chemical reactions enabled by energetic radiation?

The source of Ariel's CO_2 is unknown. Primordial carbon-containing compounds such as methane (e.g., Pollack *et al.* 1991) could possibly contribute to radiolytic production of CO_2 in combination with Ariel's H_2O ice (Delitsky and Lane 1998). Carbonaceous material delivered via impacting dust or larger particles could be another source of carbon. Indigenous CO_2 could have been produced in Ariel's interior during an early tidal heading episode and subsequently erupted onto the surface (e.g., Squyres *et al.* 1985; Shock and McKinnon 1993). The implantation of carbon ions from the Uranian magnetosphere appears to be a less likely source, as the Voyager spacecraft found almost no ions heavier

than protons during the 1986 flyby (Bridge *et al.* 1986; Krimigis *et al.* 1986). However, the seasonal dependence of heavy ion abundances is uncertain.

If radiolysis is producing CO_2 from H_2O and some source of carbon within Ariel's surface, or is acting on extant CO_2 and H_2O ices, other reaction products could be produced as well. Searches for their absorption bands could offer a sensitive probe of the chemical pathways active within Ariel's surface ices. Additional species one might expect to see include volatiles such as CO and O_2, but unless they are trapped within the host water ice (i.e., via hydrogen bonding) these species could relatively quickly escape to space. They could conceivably be detectable in the gas phase, however, if residence times are long enough and production rates are high enough. Less volatile and more chemically interesting candidates to search for include carbon suboxide C_3O_2 and its polymers $(C_3O_2)_n$, carbonic acid H_2CO_3, hydrogen peroxide H_2O_2, formaldehyde H_2CO and its polymer polyoxymethylene, and methanol CH_3OH (e.g., Schutte *et al.* 1993; Gerakines *et al.* 1996; Brucato *et al.* 1997; Delitsky and Lane 1997; Johnson and Quickenden 1997; Delitsky and Lane 1998; Gerakines and Moore 2001; Hudson and Moore 2001). Perhaps some of these compounds could survive long enough in Ariel's near-surface environment to be spectroscopically observable.

The vapor pressure of CO_2 ice at our measured H_2O ice temperature of 70 K is comparable to that of water ice at 130 K (Brown and Ziegler 1979). Ariel's darker regions may reach subsolar temperatures approaching 90 K. At these temperatures, CO_2 ice should be rapidly transformed (or even removed altogether) by volatile transport processes such as sublimation, grain growth, sintering, and solar gardening (e.g., Clark *et al.* 1983; Spencer 1987; Grundy and Stansberry 2000). Even at the lower temperatures which prevail in higher albedo regions and away from Ariel's subsolar point, CO_2 ice is considerably more readily mobilized than H_2O ice is via charged particle sputtering (e.g., Johnson *et al.* 1983),

so its longevity at the surface could be relatively brief. Alternatively, Ariel's CO_2 could be trapped within a H_2O ice matrix, making it less mobile but more readily available for carbon, oxygen, and hydrogen chemistry. However, if the CO_2 were trapped in a H_2O matrix, one would expect its absorption bands to shift in wavelength, and normally inactive modes could become activated and produce bands, such as the $2\nu_3$ transition which might be expected to produce a band near 2.14 μm (Schmitt, personal communication 2002). No convincing spectral evidence is seen for CO_2 being trapped in H_2O. Much additional work is clearly needed to work out the origin and the fate of CO_2 on Ariel's surface.

We generated synthetic spectra with the Hapke model (e.g., Hapke 1993) to estimate the quantity of CO_2 ice required by the observed absorptions. Unfortunately, abundances derived from disk-integrated spectral models are extremely dependent on model assumptions. For this reason, it would be imprudent to assign much confidence to any abundance ratio computed from a single model. We tried four different model scenarios to illustrate the influence of model assumptions on computed abundances, using CO_2 ice refractive indices n from (G.B. Hansen, personal communication; see Hansen 1997) and absorption coefficients k from Schmitt *et al.* (1998). In the first model, we simulated a glaze of CO_2 ice atop a multiple-scattering mixture of H_2O and dark material. The best-fitting thickness of a hemispheric CO_2 glaze is about 5 μm; thicker coatings would be required for glazes not covering the entire hemisphere. In our second model, we replaced a fraction of the H_2O grains with CO_2 ice grains of the same size. Mixing ratios in the neighborhood of H_2O:CO_2=3:1 produced reasonable fits with this scenario. An alternate mixture disperses the CO_2 at the molecular level within H_2O by means of a linear combination of optical constants. This scenario yielded a similar mixing ratio of H_2O:CO_2=4:1. Finally, we tried an areal mixture, in which H_2O ice was replaced with CO_2 ice on a fraction of Ariel's trailing hemisphere. In this model (the one shown in Fig. 2), CO_2 ice covering 8% of the trailing hemisphere duplicated the observed bands reasonably well. Thus a relatively small

region could be responsible for the observed absorption and it could easily be confined to the hemisphere not observed by Voyager, which has recently become illuminated by the sun after a long seasonal polar winter night.

On Ariel's leading hemisphere, we see no convincing evidence for absorption by CO_2 ice. A slight dip does appear near 1.965 μm in our leading hemisphere spectrum. This wavelength is not quite where the CO_2 ice $2\nu_1+\nu_3$ band should be and we see no corresponding features near 2.012 or 2.070 μm where the noise characteristics of our data are much better. We believe the 1.965 μm dip to be spurious, probably a residual feature from imperfect cancellation of telluric absorptions. Using the four model configurations described earlier, we derived approximate upper limits on CO_2 ice for Ariel's leading hemisphere. For the glaze model, an upper limit of 3 μm of CO_2 ice is consistent with our data. The other models place upper limits on the NH_3:H_2O mixing ratio ranging from 3% for the model having a discrete patch of CO_2 ice to 15% for the model based on linear combinations of CO_2 and H_2O ice optical constants.

Finally, we turn to the question of ammonia. NH_3 has perennially been sought on icy outer solar system surfaces, but has yet to be convincingly identified in spite of possessing several strong, distinctive near-infrared absorption bands, chiefly near 2.0 μm and between 2.20 and 2.25 μm (precise wavelengths and band shapes depend on the hydration state of the NH_3). No evidence is seen in our data for any NH_3 absorption near 2 μm (see Fig. 2) or near 2.2 μm (Fig. 3).

EDITOR: Please place FIGURE 3 near here.

As we did earlier for CO_2 ice, we used our four model scenarios to set approximate upper limits for NH_3 on Ariel. The maximum admissible global glaze thickness is about 0.1 μm, and upper limits on the mixing ratio of NH_3:H_2O ranged from 0.1% to 2% for our

collection of model scenarios. Likewise for ammonia monohydrate, we derive an upper limit global glaze thickness of about 1 μm, and upper limit mixing ratios relative to H_2O from 1% to 4%. To construct these models, we used NH_3 ice optical constants from Sill *et al.* (1980, unfortunately only available at inadequately low spectral resolution) and ammonia monohydrate optical constants from Schmitt *et al.* (1998).

4. Conclusion

We report the discovery of two important spectral differences between the leading and trailing hemispheres of the Uranian satellite Ariel. First, the H_2O ice absorption bands are deeper in the leading hemisphere spectrum. This spectral pattern is similar to leading-trailing asymmetries observed on many Jovian and Saturnian icy satellites. Second, three absorption bands of CO_2 ice appear in the trailing hemisphere's spectrum. The detection of CO_2 ice finally confirms the long-suspected presence of carbon at Ariel's surface (e.g., Smith *et al.* 1986) and also hints at its chemical interaction with the ubiquitous H_2O ice.

Acknowledgments: We thank W. Golisch, D. Griep, S.J. Bus, J.T. Rayner, and K. Crane for assistance with the telescope and with SpeX, M.W. Buie and R.S. Bussmann for contributing to the reduction pipeline, C.A. Hibbitts, A.S. Rivkin, B. Schmitt, and R.E. Johnson for stimulating discussions, G.B. Hansen and S.A. Stern for constructive and insightful reviews, and NASA for its support of the IRTF. This work was made possible by National Science Foundation grant AST-0085614 to E.F. Young at Southwest Research Institute and NASA Planetary Geology and Geophysics grant NAG5-10159 to W.M. Grundy at Lowell Observatory.

REFERENCES

Bertie, J.E., and E. Whalley 1964. Infrared spectra of ices I_h and I_c in the range 4000 to 350 cm^{-1}. *J. Chem. Phys.* **40,** 1637-1645.

Bertie, J.E., and S.M. Jacobs 1977. Far-infrared absorption by ices I_h and I_c at 4.3 K and the power diffraction pattern of ice I_c. *J. Chem. Phys.* **67,** 2445-2448.

Bridge, H.S., J.W. Belcher, B. Coppi, A.J. Lazarus, R.L. McNutt Jr., S. Olbert, J.S. Richardson, M.R. Sands, R.S. Selesnick, J.D. Sullivan, R.E. Hartle, K.W. Ogilvie, E.C. Sittler Jr., F. Bagenal, R.S. Wolff, V.M. Vasyliunas, G.L. Siscoe, C.K. Goertz, and A. Eviatar 1986. Plasma observations near Uranus: Initial results from Voyager 2. *Science* **233,** 89-93.

Brown, R.H., and D.P. Cruikshank 1983. The Uranian satellites: Surface compositions and opposition brightness surges. *Icarus* **55,** 83-92.

Brown, G.N. Jr., and W.T. Ziegler 1979. Vapor pressure and heats of vaporization and sublimation of liquids and solids of interest in cryogenics below 1–atm pressure. *Adv. Cryogenic Eng.* **25**, 662-670.

Brucato, J.R., M.E. Palumbo, and G. Strazzula 1997. Carbonic acid by ion implantation in water/carbon dioxide ice mixtures. *Icarus* **125,** 135-144.

Buie, M.W., and W.M. Grundy 2000. The distribution and physical state of H_2O on Charon. *Icarus* **148,** 324-339.

Buratti, B.J., and J.A. Mosher 1991. Comparative global albedo and color maps of the Uranian satellites. *Icarus* **90,** 1-13.

Calvin, W.M., and R.N. Clark 1993. Spectral distinctions between the leading and trailing hemispheres of Callisto: New observations. *Icarus* **104,** 69-78.

Cheng, A.F., S.M. Krimigis, and L.J. Lanzerotti 1991. Energetic particles at Uranus. In *Uranus*, University of Arizona Press, Tucson.

Clark, R.N., F.P. Fanale, and A.P. Zent 1983. Frost grain size metamorphism: Implications for remote sensing of planetary surfaces. *Icarus* **56,** 233-245.

Clark, R.N., R.H. Brown, P.D. Owensby, and A. Steele 1984. Saturn's satellites: Near-infrared spectrophotometry (0.65-2.5 microns) of the leading and trailing sides and compositional implications. *Icarus* **58,** 265-281.

Croft, S.K., and L.A. Soderblom 1991. Geology of the Uranian satellites. In *Uranus*, University of Arizona Press, Tucson.

Cruikshank, D.P., and J. Apt 1984. Methane on Triton: Physical state and distribution. *Icarus* **58,** 306-311.

Cruikshank, D.P., and R.H. Brown 1981. The Uranian satellites: Water ice on Ariel and Umbriel. *Icarus* **45,** 607-611.

Cruikshank, D.P., T.L. Roush, T.C. Owen, T.R. Geballe, C. de Bergh, B. Schmitt, R.H. Brown, and M.J. Bartholomew 1993. Ices on the surface of Triton. *Science* **261,** 742-745.

Delitsky, M.L., and A.L. Lane 1997. Chemical schemes for surface modification of icy satellites: A road map. *J. Geophys. Res.* **102,** 16385-16390.

Delitsky, M.L., and A.L. Lane 1998. Ice chemistry on the Galilean satellites. *J. Geophys. Res.* **103,** 31391-31403.

Dumas, C., R.J. Terrile, R.H. Brown, G. Schneider, and B.A. Smith 2001. Hubble space telescope NICMOS spectroscopy of Charon's leading and trailing hemispheres. *Astron. J.* **121,** 1163-1170.

Eviatar, A., and J.D. Richardson 1986. Predicted satellite plasma tori in the magnetosphere of Uranus. *Astrophys. J.* **300,** L99-L102.

Fink, U., and H.P. Larson 1975. Temperature dependence of the water-ice spectrum between 1 and 4 microns: Application to Europa, Ganymede, and Saturn's rings. *Icarus* **24,** 411-420.

Gerakines, P.A., and M.H. Moore 2001. Carbon suboxide in astrophysical ice analogs. *Icarus* **154,** 372-380.

Gerakines, P.A., W.A. Schutte, and P. Ehrenfreund 1996. Ultraviolet processing of interstellar ice analogs I.: Pure ices. *Astron. Astrophys.* **312,** 289-305.

Grundy, W.M., and M.W. Buie 2002. Spectroscopy of Pluto and Triton at 3-4 microns: Possible evidence for wide distribution of non-volatile solids. *Astron. J.* **124,** 2273-2278.

Grundy, W.M., and B. Schmitt 1998. The temperature-dependent near-infrared absorption spectrum of hexagonal H_2O ice. *J. Geophys. Res.* **103,** 25809-25822.

Grundy, W.M., and J.A. Stansberry 2000. Solar gardening and the seasonal evolution of nitrogen ice on Triton and Pluto. *Icarus* **148,** 340-346.

Grundy W.M., M.W. Buie, J.A. Stansberry, J.R. Spencer, and B. Schmitt 1999. Near-infrared spectra of icy outer solar system surfaces: Remote determination of H_2O ice temperatures. *Icarus* **142,** 536-549.

Hansen, G.B. 1997. The infrared absorption spectrum of carbon dioxide ice from 1.8 to 333 microns. *J. Geophys. Res.* **102,** 21569-21587.

Hapke, B. 1993. *Theory of reflectance and emittance spectroscopy.* Cambridge University Press, New York.

Hibbitts, C.A., T.B. McCord, and G.B. Hansen 2000. Distributions of CO_2 and SO_2 on the surface of Callisto. *J. Geophys. Res.* **105,** 22541-22557.

Horne, K. 1986. An optimal extraction algorithm for CCD spectroscopy. *PASP* **98,** 609-617.

Hudson, R.L., and M.H. Moore 2001. Radiation chemical alterations in solar system ices: An overview. *J. Geophys. Res.* **106,** 33275-33284.

Johnson, R.E. 1990. Energetic charged-particle interactions with atmospheres and surfaces. Springer-Verlag, New York.

Johnson, R.E., and T.I. Quickenden 1997. Photolysis and radiolysis of water ice on outer solar system bodies. *J. Geophys. Res.* **102,** 10985-10996.

Johnson, R.E., L.J. Lanzerotti, W.L. Brown, W.M. Augustyniak, and C. Mussil 1983. Charged particle erosion of frozen volatiles in ice grains and comets. *Astron. Astrophys.* **123,** 343-346.

Karkoschka, E. 1997. Rings and satellites of Uranus: Colorful and not so dark. *Icarus* **125,** 348-363.

Kieffer, H.H., and W.D. Smythe 1974. Frost spectra: Comparison with Jupiter's satellites. *Icarus* **21,** 506-512.

Krimigis, S.M., T.P. Armstrong, W.I. Axford, A.F. Cheng, G. Gloeckler, D.C. Hamilton, E.P. Keath, L.J. Lanzerotti, and B.H. Mauk 1986. The magnetosphere of Uranus: Hot plasma and radiation environment. *Science* **233,** 97-102.

Lanzerotti, L.J., W.B. Brown, C.G. Maclennan, A.F. Cheng, S.M. Krimigis, and R.E. Johnson 1987. Effects of charged particles on the surfaces of the satellites of Uranus. *J. Geophys. Res.* **92,** 14949-14957.

McCord, T.B., R.W. Carlson, W.D. Smythe, G.B. Hansen, R.N. Clark, C.A. Hibbitts, F.P. Fanale, J.C. Granahan, M. Segura, D.L. Matson, T.V. Johnson, and P.D. Martin 1997. Organics and other molecules in the surfaces of Callisto and Ganymede. *Science* **278,** 271-275.

McCord, T.B., G.B. Hansen, R.N. Clark, P.D. Martin, C.A. Hibbitts, F.P. Fanale, J.C. Granahan, M. Segura, D.L. Matson, T.V. Johnson, R.W. Carlson, W.D. Smythe, G.E. Danielson, and the NIMS team 1998. Non-water-ice constituents in the surface material of the icy Galilean satellites from the Galileo near-infrared mapping spectrometer investigation. *J. Geophys. Res.* **103,** 8603-8626.

Ness, N.F., M.H. Acuña, K.W. Behannon, L.F. Burlaga, J.E.P. Connerney, R.P. Lepping, and F.M. Neubauer 1986. Magnetic fields at Uranus. *Science* **233,** 85-89.

Plescia, J.B. 1987. Geological terrains and crater frequencies on Ariel. *Nature* **327,** 201-204.

Pospieszalska, M.K., and R.E. Johnson 1989. Magnetospheric ion bombardment profiles of satellites: Europa and Dione. *Icarus* **78,** 1-13.

Pollack, J.B., J.I. Lunine, and W.C. Tittemore 1991. Origin of the Uranian satellites. In *Uranus*, University of Arizona Press, Tucson.

Quirico, E., and B. Schmitt 1997. Near-infrared spectroscopy of simple hydrocarbons and carbon oxides diluted in solid N_2 and as pure ices: Implications for Triton and Pluto. *Icarus* **127,** 354-378.

Quirico, E., S. Douté, B. Schmitt, C. de Bergh, D.P. Cruikshank, T.C. Owen, T.R. Geballe, and T.L. Roush 1999. Composition, physical state, and distribution of ices at the surface of Triton. *Icarus* **139,** 159-178.

Rayner, J.T., D.W. Toomey, P.M. Onaka, A.J. Denault, W.E. Stahlberger, D.Y. Watanabe, and S.I. Wang 1998. SpeX: A medium-resolution IR spectrograph for IRTF. *Proc. SPIE* **3354,** 468-479.

Schmitt, B., E. Quirico, F. Trotta, and W.M. Grundy 1998. Optical properties of ices from UV to infrared. In *Solar System Ices*, Kluwer Academic Publishers, Boston.

Schutte, W.A., L.J. Allamandola, and S.A. Sandford 1993. An experimental study of the organic molecules produced in cometary and interstellar ice analogs by thermal formaldehyde reactions. *Icarus* **104,** 118-137.

Shock, E.L., and W.B. McKinnon 1993. Hydrothermal processing of cometary volatiles: Applications to Triton. *Icarus* **106,** 464-477.

Sill, G., U. Fink, and J.R. Ferraro 1980. Absorption coefficients of solid NH_3 from 50 to 7000 cm^{-1}. *J. Opt. Soc. Am.* **70,** 724-739.

Smith, B.A., L.A. Soderblom, R. Beebe, D. Bliss, J.M. Boyce, A. Brahic, G.A. Briggs, R.H. Brown, S.A. Collins, A.F. Cook II, S.K. Croft, J.N. Cuzzi, G.E. Danielson, M.E. Davies, T.E. Dowling, D. Godfrey, C.J. Hansen, C. Harris, G.E. Hunt, A.P. Ingersoll, T.V. Johnson, R.J. Krauss, H. Masursky, D. Morrison, T. Owen, J.B. Plescia, J.B. Pollack, C.C. Porco, K. Rages, C. Sagan, E.M. Shoemaker, L.A. Sromovsky, C. Stoker, R.G. Strom, V.E. Suomi, S.P. Synnott, R.J. Terrile, P. Thomas, W.R. Thompson, and J. Veverka 1986. Voyager 2 in the Uranian system: Imaging science results. *Science* **233,** 43-64.

Spencer, J.R. 1987. Thermal segregation of water ice on the Galilean satellites. *Icarus* **69,** 297-313.

Squyres, S.W., R.T. Reynolds, and J.J. Lissauer 1985. The enigma of the Uranian satellites' orbital eccentricities. *Icarus* **61,** 218-223.

Veverka, J., R.H. Brown, and J.F. Bell 1991. Uranus satellites: Surface properties. In *Uranus*, University of Arizona Press, Tucson.

Zahnle, K., P. Schenk, S. Sobieszczyk, L. Dones, and H.F. Levison 2001. Differential cratering of synchronously rotating satellites by ecliptic comets. *Icarus* **153,** 111-129.

FIGURE CAPTIONS

Fig. 1.— Spectral observations of Ariel's leading and trailing hemispheres reveal deeper H_2O ice I absorption bands on the leading hemisphere (July 17). One spectrum is shifted upward by 0.1 while the other is shifted downward by the same amount.

Fig. 2.— CO_2 ice absorption bands as seen in the spectrum of Triton (arbitrarily scaled), in a simple multiple-scattering model, and on the trailing hemisphere of Ariel (2002 July 16, offset by +0.1), but not on Ariel's leading hemisphere (2002 July 17, offset by −0.1). The top curve is a telluric transmission spectrum produced by dividing a solar analog star spectrum observed through a high airmass by a spectrum obtained at a lower airmass (arbitrarily scaled). The shapes of the telluric CO_2 vapor absorption bands differ considerably from the CO_2 ice features. Identification of the CO_2 ice transitions is from Quirico and Schmitt (1997).

Fig. 3.— Non-detection of absorption bands of NH_3 or its monohydrate near 2.22 μm, as shown by Hapke models having 2 to 3 times the upper limit quantities discussed in the text (smooth curves). Each set of spectra was shifted by 0.05, one upward and one downward. A_1 is the albedo at a 1° phase angle (e.g., Buie and Grundy 2000). The scaling is based on 0.91 μm photometry by Karkoschka (1997).

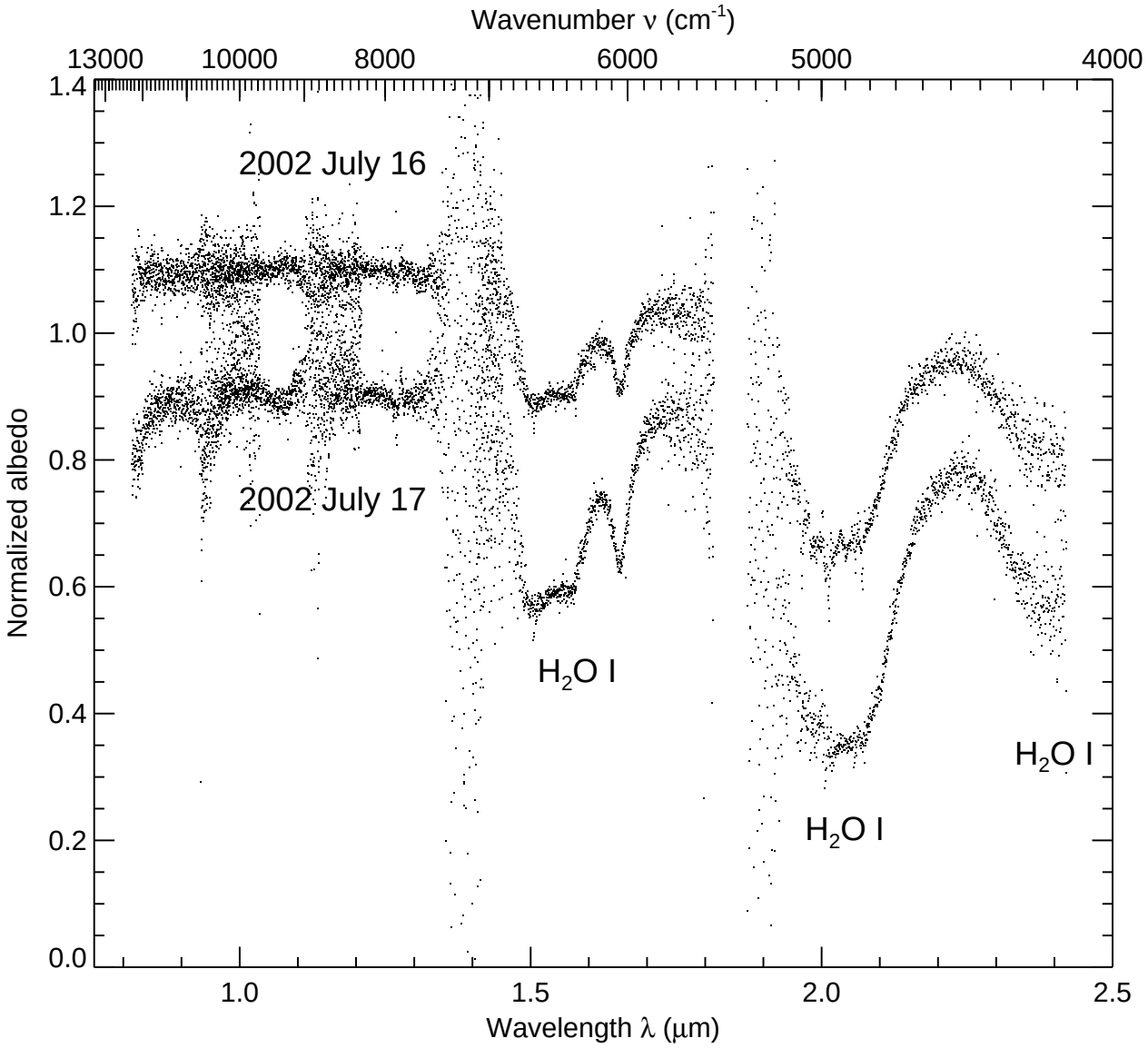

Fig. 1.— Spectral observations of Ariel's leading and trailing hemispheres reveal deeper H_2O ice I absorption bands on the leading hemisphere (July 17). One spectrum is shifted upward by 0.1 while the other is shifted downward by the same amount.

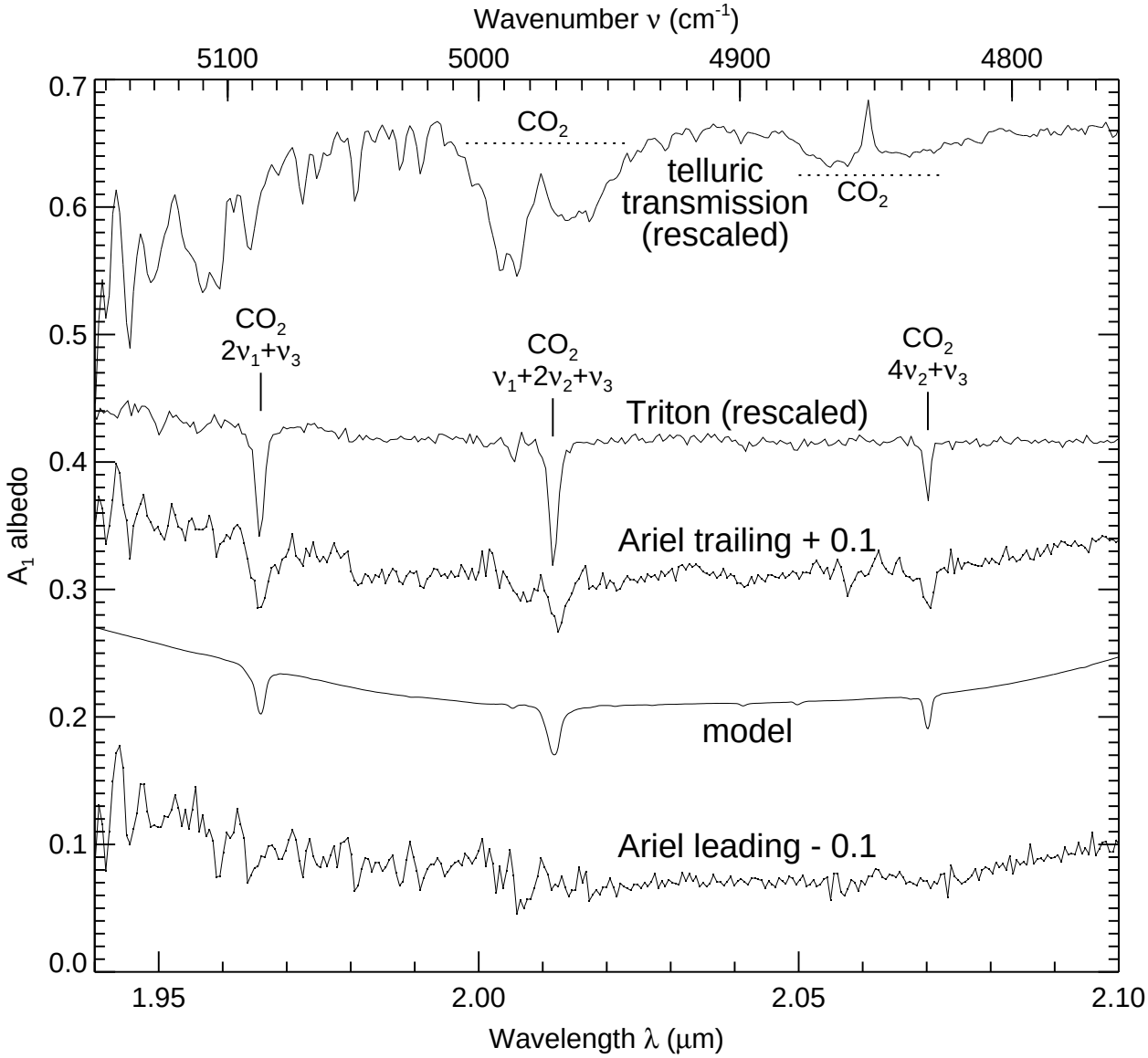

Fig. 2.— CO_2 ice absorption bands as seen in the spectrum of Triton (arbitrarily scaled), in a simple multiple-scattering model, and on the trailing hemisphere of Ariel (2002 July 16, offset by +0.1), but not on Ariel's leading hemisphere (2002 July 17, offset by −0.1). The top curve is a telluric transmission spectrum produced by dividing a solar analog star spectrum observed through a high airmass by a spectrum obtained at a lower airmass (arbitrarily scaled). The shapes of the telluric CO_2 vapor absorption bands differ considerably from the CO_2 ice features. Identification of the CO_2 ice transitions is from Quirico and Schmitt (1997).

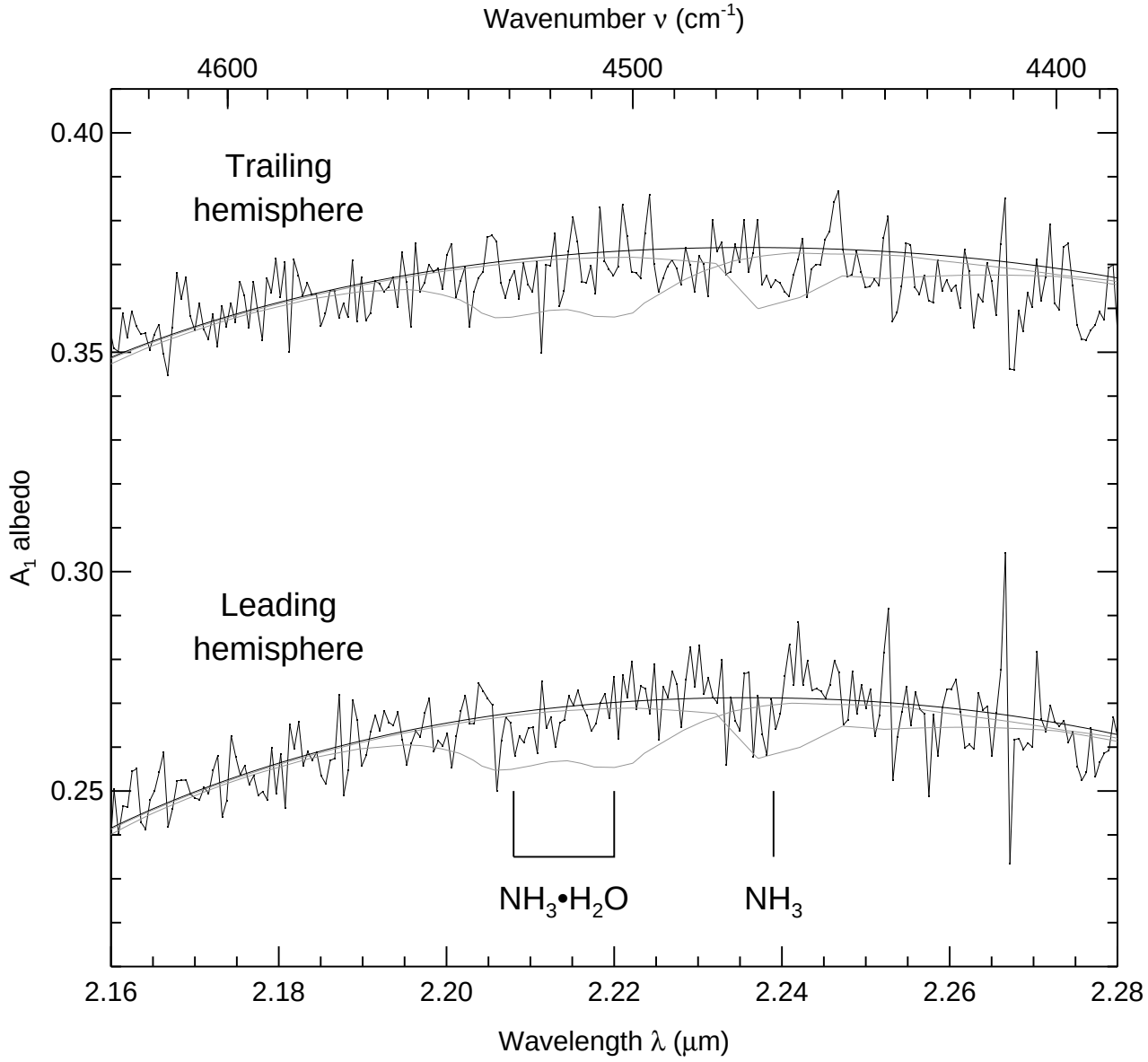

Fig. 3.— Non-detection of absorption bands of NH_3 or its monohydrate near 2.22 μm, as shown by Hapke models having 2 to 3 times the upper limit quantities discussed in the text (smooth curves). Each set of spectra was shifted by 0.05, one upward and one downward. A_1 is the albedo at a 1° phase angle (e.g., Buie and Grundy 2000). The scaling is based on 0.91 μm photometry by Karkoschka (1997).